Available online at www.sciencedirect.com
SCIENCE DIRECT®
Journal of Organometallic Chemistry 690 (2005) 6300–6308
Journal of Organometallic Chemistry
www.elsevier.com/locate/jorganchem

Synthesis and application of functional polyethylene graft copolymers by atom transfer radical polymerization

Jyh-Ming Hwu [a], Ming-Jen Chang [b], Jui-Chi Lin [b], Hsiu-Yu Cheng [b], George-J Jiang [b,*]

[a] *Union Chemical Laboratories, Industrial Technology Research Institute, Hsinchu 300, Taiwan, ROC*
[b] *Department of Chemistry, Chung Yuan Christian University, Pu-Chung Li, Pu-Jen 22, Chung Li, Taiwan, ROC*

Received 1 November 2004; received in revised form 27 January 2005; accepted 18 April 2005
Available online 29 September 2005

Abstract

This investigation attempts to elucidate the copolymerization reaction ethylene and *p*-methylstyrene via the homogeneous metallocene catalyst, $Et(Ind)_2ZrCl_2$. With increasing of *p*-methylstyrene concentration, the poly[ethylene-*co*-(*p*-methylstyrene)] copolymer shows systematical decrease of melting temperature and crystallinity and increase of glass transition temperature. The benzylic protons of *p*-methylstyrene are ready for numerous chemical reactions, such as halogenation and oxidation, which can introduce functional groups at the *p*-methyl group position under mild reaction conditions. With the bromination reaction of poly[ethylene-*co*-(*p*-methylstyrene)], polyethylene graft copolymers, such as polyethylene-*g*-poly(methyl methacrylate) and polyethylene-*g*-polystyrene can be prepared via atomic transfer radical polymerization. The following selective bromination reaction of *p*-methylstyrene units in the copolymer and the subsequent radical graft-from polymerization were effective methods of producing polymeric side chains with well-defined structure. The products were characterized by nuclear magnetic resonance, gel-permeation chromatography, differential scanning calorimetry, and thermal gravimetric analysis. Additionally, the morphology of PE/PMMA and PE/PMMA/PE-*g*-PMMA blend are compared by using scanning electron microscope.

Keywords: Metallocene; Atom transfer radical polymerization; Polyethylene

1. Introduction

For many decades since the commercialization of PE and PP, The functionalization of polyolefins has been scientifically interesting and technologically important research subject, with the mainfocus being on improving the adhesion and compatibility with other materials [1,2]. Unfortunately, the chemistry for preparing functional polyolefins is very limited both in the direct and post polymerization process, namely owing to the catalyst poison and the inert nature of polyolefins [3,4]. Recently, several new research approaches have been conducted, including the use of late transition metals and protecting group [5–7]. The use of graft and block copolymers as emulsifiers and interfacial compatibilizers is an established technique for improving polymer interaction and morphology in polymer blends [8,9]. In most cases, the products were not well characterized, especially the microstructure of the resulting graft copolymer. As expected, this graft polymerization process produced considerable amounts of ungrafted homopolymers and potentially some cross-linking products.

In our previous investigation on the preparation of polyolefin graft copolymers, the transformation process was implemented via the reactive polyolefins [10–15]. In other words, the process involves the transition metal catalysts copolymerization to produce polyolefin copolymer containing reactive comonomer units, which can be transformed to initiators for graft-from polymerization. To be successful, the transformation reaction must be effective and selective to produce the initiation

* Corresponding author. Tel.: +886-3-2652001; fax: +886-3-2652099.
E-mail address: george@cycu.edu.tw (George-J. Jiang).

0022-328X/$ - see front matter © 2005 Elsevier B.V. All rights reserved.
doi:10.1016/j.jorganchem.2005.04.043

site only in the comonomer units of the polyolefin backbone. In addition, the resulting polymeric initiators must be sufficiently stable for the following graft-from polymerization that is essential to prevent side reactions, such as cross-linking and homopolymerization.

Recently, Chung et al. [16–19] extended the new type reactive comonomer, e.g., methylstyrene. The main advantages of methylstyrene are due to its commercial availability, easy incorporation into polyolefin and versatility in functionalization chemistry under various reaction mechanisms like free radical and anionic processes. The benzylic protons are known to be facile in numerous chemical reactions, such as halogenation [20], metallation [21], and oxidation [22], to form desirable functional groups at the benzylic position under mild reaction conditions. Additionally, the benzylic protons can also be interconverted to stable free radical or anionic initiator for graft-form polymerization [23].

Atom transfer radical addition, ATRA, is an efficient technique for carbon–carbon bond formation in organic synthesis and many benefits of this method are now well recognized [24]. In some of these reactions, a transition metal catalyst acts as a carrier of the halogen atom in a reversible redox process [25]. Initially, the transition metal species, M^n, abstracts halogen atom X from the organic halide, RX, to form the oxidized species, $M^{n+1}X$ and the carbon-centered radical R·. In the subsequent step, the radical R· participates in an inter or intramolecular radical addition to alkene, Z, with the formation of the intermediate radical species, RZ·. The reaction between $M^{n+1}X$ and RZ· results in a target product, RZX, and regenerates the reduced transition metal species, Mn, that further promotes a new redox process. The fast reaction between RZ· and $M^{n+1}X$ apparently suppresses bimolecular termination between alkyl radicals and efficiently introduces a halogen functional group X into the final product with good to excellent yield. One of the most successful controlled/living radical polymerization methods developed is atom transfer radical polymerization (ATRP) which has its roots in ATRA [26,27]. ATRP has been proven to be effective for a wide range of monomers and appears a powerful tool for the polymer chemist, providing new possibilities in structural and architectural design and allowing the development of new materials with monomers currently available.

This study presents the preparation of grafted PE with styrene, methyl methacrylate and *n*-butyl acrylate via the ATRP method using a macroinitiator of bromination poly[ethylene-*co*-(*p*-methylstyrene)] (Scheme 1). The following selective bromination of poly[ethylene-*co*-(*p*-methylstyrene)] units in the copolymer and the subsequent radical graft-form polymerization were effective to produce polymeric side chain with well-defined structure. In the bulk, the individual PE and functionalized polymer segments in the polymer blend are phase-separated. The microscopy studies reveal the

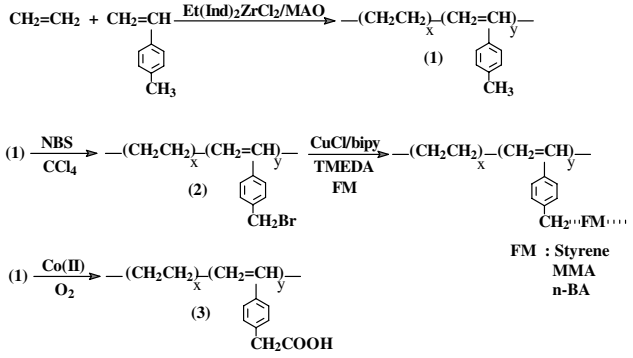

Scheme 1.

effectiveness of the addition of PE-*g*-functionalized polymer in the polymer, specifically in improving the dispersion, reducing the phase sizes and increasing interfacial interaction between domains.

2. Experimental

2.1. Material

p-Methylstyrene (MS), methyl methacrylate (MMA) and *t*-butyl acrylate (BA) were dried over calcium hydride before distillation. *N*-hexane and toluene were deoxygenated by nitrogen purging before refluxing for 48 h and distilled over sodium. Metallocene compounds, methylaluminoxane, copper (I) chloride, 2,2-dipyridyl, cobalt (II) acetate tetrahydrate, sodium bromide and acetic acid were obtained from Aldrich Co. Ltd. Finally, ethylene gas was sourced from Jian Reeng Gases Co., Taiwan.

2.2. Instruments

The FT-IR spectrum was measured using Bio-Rad FTS-7 that cast on KBr. The ^{1}H- and ^{13}C NMR spectrum were measured in 1,1,2,2-tetrachloroethane-d_2 at 90 °C using a Buchi 300 NMR spectrometer. The molecular weight and molecular weight distribution were obtained by high temperature gel-permeation chromatography (GPC) at 120 °C using 1,3,5-trichlorobenzene as a solvent and then were calibrated with stand polystyrene samples. The melting temperature, enthalpy and glass-transition temperature were measured with a Sekio DSC-200 calorimeter at a heating rate of 20 °C/min. The decomposition temperature (T_d) was got from a Sekio TG-DTA 5200 calorimeter at a heating rate of 20 °C/min. Meanwhile the scanning electron microscopy (SEM) image of gold-coated polymer powders was recorded using JSM-6300, JEOL with an acceleration voltage of 20 KV.

2.3. Copolymerization of ethylene and p-methylstyrene

The *p*-methylstyrene was mixed with solvent and methylaluminoxane (10 wt% in toluene) needed in a Parr 250 ml stainless autoclave equipped with a mechanical stirrer. The sealed reactor was saturated with 40 psi ethylene at 40 °C before adding the catalyst solution to initiate the polymerization. After 1 h, the reaction was terminated by adding 100 ml of dilute HCl solution in methanol. Then the copolymer was isolated by filtering and washed completely with methanol and finally was dried under vacuum at room temperature for 24 h.

2.4. Bromination of poly[ethylene-co-(p-methylstyrene)]

The poly[ethylene-*co*-(*p*-methylstyrene)] was mixed with *N*-bromosuccinimide (NBA) and 2,2′-azoisobutyronitrile (AIBN) in 100 ml carbon tetrachloride at 300 ml glass reactor with magnetic stirrer. This reaction was refluxed by nitrogen for 20 min and terminated with adding to the methanol. The yellow bromination copolymer was obtained by filtering and washed completely with methanol and dried under vacuum at room temperature for 24 h.

2.5. Graft copolymerization of poly[ethylene-co-(p-methylstyrene)]

The graft copolymerization was performed in a sealed glass reactor. To a glass reactor, poly[ethylene-*co*-(*p*-methylstyrene)], copper (I) chloride (CuCl) and 2,2-dipyridyl (dpy) were weighed under ambient atmosphere. The distilled methyl methacrylate (or *t*-butyl acrylate) and toluene were added using syringe under nitrogen atmosphere. After three freeze-pump-thaw cycles, the glass reactor was under vacuum sealed and the reaction mixture was heated at 100 °C for 24 h. The reaction mixture was precipitated in methanol and washed completely with methanol and dried under vacuum at room temperature for 24 h. The reaction mixture was precipitated in MeOH and washed completely with MeOH and dried under vacuum at room temperature for 24 h. Acetone is a good solvent for PMMA and PBA homopolymers that was used during fractionation, using a Soxhlet apparatus under nitrogen for 24 h. The soluble fractions were isolated by vacuum removal of solvent. The major insoluble fraction was PE graft copolymer.

3. Results and discussion

3.1. Properties of poly[ethylene-co-(p-methylstyrene)] by using metallocene catalysts

Six metallocene catalysts, including Ti, Zr and Hf center metals, were used in this copolymerization. Table 1 shows more *p*-MS comonomers incorporation to the polyethylene main chain by *rac*-Et(Ind)$_2$ZrCl$_2$ and Cp$_2$HfCl$_2$ catalysts in the same reaction condition. Cp$_2$MCl$_2$ catalysts, without a bridge between Cp ligands, with the zirconium active site sandwiched between two Cp rings, and with Cp–M–Cp angle of 180 °C. In bridge catalyst, like *rac*-Et(Ind)$_2$ZrCl$_2$, ethylene bridge induces the constrained indenyl ligand geometry, with Cp–Zr–Cp angle of 125.8 °C. The spatial opening of the catalytic site shall be *rac*-Et(Ind)$_2$MCl$_2$ > Cp$_2$MCl$_2$. Based on the structure and activity relationships of the metallocene catalysts, the incorporation of *p*-MS is expected to follow the same trend of spatial opening. The bridge catalyst with the spatially opened active sites is more favorable than the non-bridge catalyst. Furthermore, the size of the center metals is Hf > Zr > Ti and the *p*-MS comonomers should easily react with hafnium metal. The T_m and ΔH depended on the PMS components in the copolymer. The P[E-*co*-(*p*-MS)] displayed lower T_m and ΔH with increasing the *p*-MS incorporation to the polyethylene. A special situation exists with CpTiCl$_3$ (A-1, Table 1) in the P[E-*co*-(*p*-MS)] copolymerization. This catalyst can polymerizate with *p*-methylstyrene to obtain the poly(*p*-methylstyrene) and it would form more homopolymers or block copolymers in this copolymerization (Fig. 1). Significantly, the differential scanning calorimetry (DSC) curve of Fig. 2 contained two melting points (120.8 and 73.8 °C when using CpTiCl$_3$/MAO catalyst.

Table 1
Properties of PE-*co*-PMS by using different metallocene catalysts[a]

No.	Catalyst (10 μmol)	Yield (g)	PMS[b] (mol%)	T_m (°C)	ΔH (J/g)
A-1	CpTiCl$_3$	0.33	20.5[c]	120.8, 73.8	20.8, 44.8
A-2	(Ind)TiCl$_3$	0.14	1.1	132.3	119.1
A-3	Cp$_2$ZrCl$_2$	1.25	0.4	132.0	158.6
A-4	CpTpZrCl$_2$	1.91	0.9	132.0	158.7
A-5	*rac*-Et(Ind)$_2$ZrCl$_2$	2.02	4.9	118.6	131.0
A-6	Cp$_2$HfCl$_2$	1.73	3.8	125.2	134.0

[a] MAO = 10 mmol, *p*-methylstyrene = 30 mmol, toluene = 100 ml, ethylene pressure = 40 psi, polymerization temperature = 40 °C, polymerization time = 1 h.
[b] PMS components in the copolymer were detected by ^{1}H NMR.
[c] Including homopolymer and copolymer (ratio = 9.1/1).

The copolymers were firstly analyzed by GPC and ^{1}H NMR measurements. Fig. 3 shows the typical GPC curves of the PE and P[E-*co*-(*p*-MS)] prepared by *rac*-Et(Ind)$_2$ZrCl$_2$/MAO catalyst. The GPC curves show a slight reduction of molecular weight and molecular weight distribution in the copolymer. The better diffusibility of monomers in the copolymer structures (lower crystallinity) may help to provide the ideal polymerization condition. Notably, the average molecular weight of copolymers maintains a content value throughout

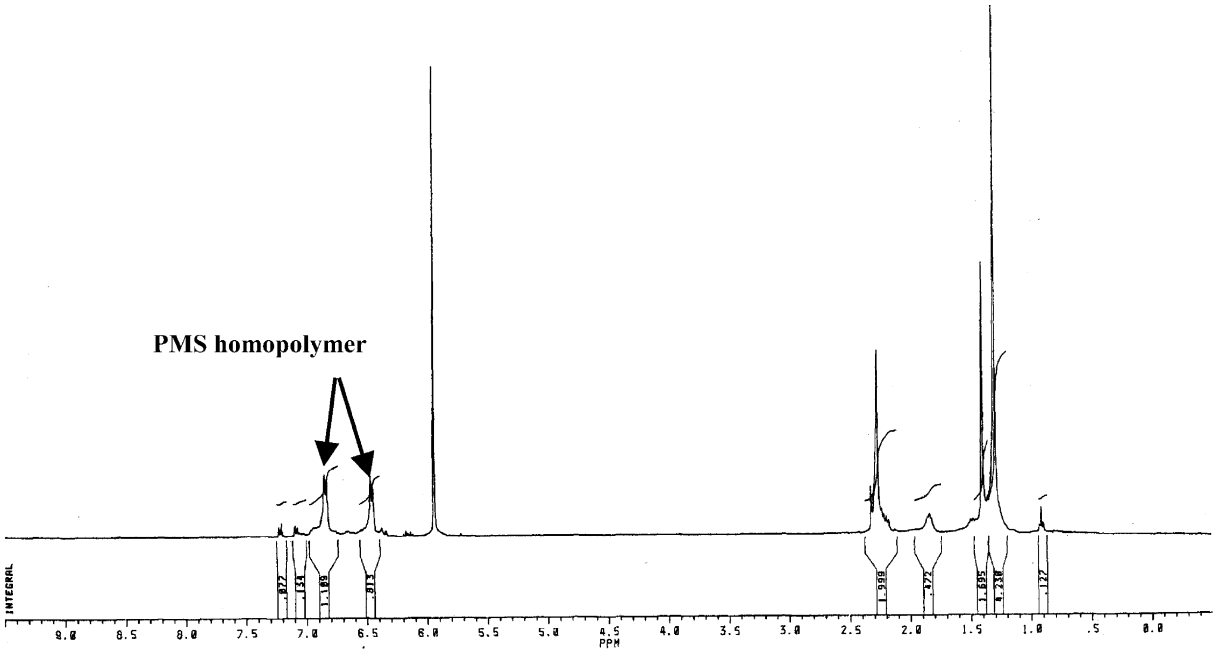

Fig. 1. The ^{1}H NMR spectrum of PE-*co*-PMS by using $CpTiCl_3$ catalyst.

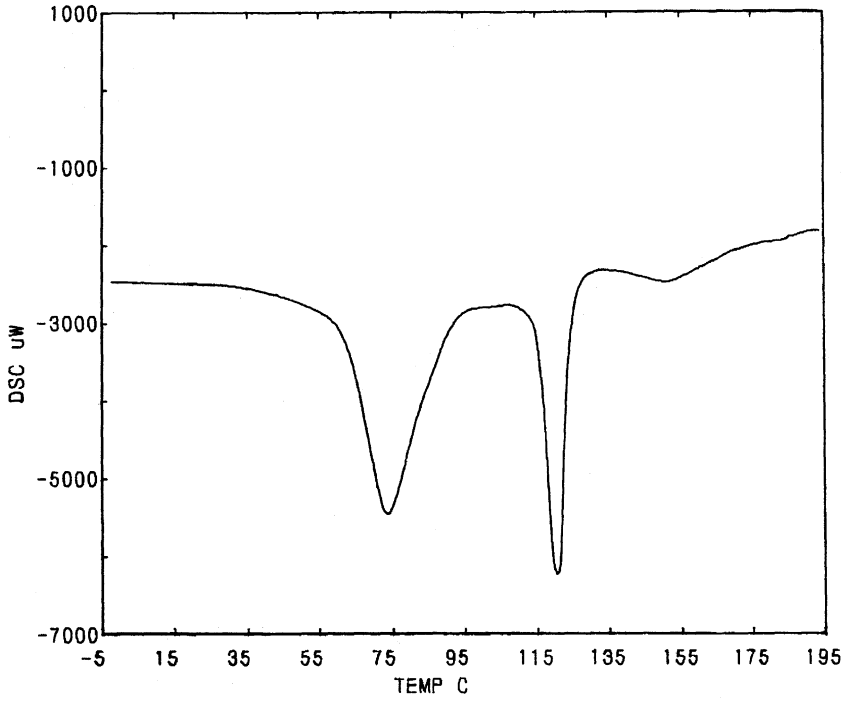

Fig. 2. The DSC curve of PE-*co*-PMS by using $CpTiCl_3$ catalyst.

the entire composition range, which can be attributed to the relatively high reactivity of *p*-MS.

Fig. 4(a) illustrates the ^{1}H NMR spectrum of P[E-*co*-(*p*-MS)] copolymers, containing 4.9 mol% of PMS. Besides the major chemical shift at 1.35 ppm, corresponding to CH_2 in the main chain, three minor chemical shifts occur around 2.35, 2.5 and 7.0–7.3 ppm, corresponding to CH_3, CH and aromatic protons in

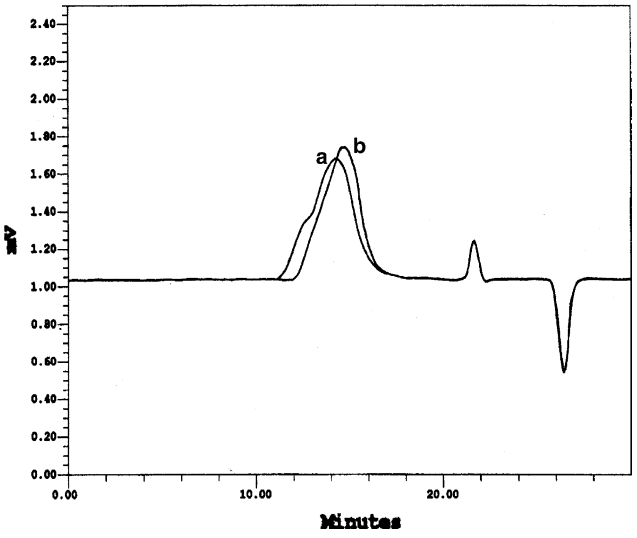

Fig. 3. The GPC curves of: (a) PE (b) PE-*co*-PMS by using *rac*-Et(Ind)$_2$ZrCl$_2$ catalyst.

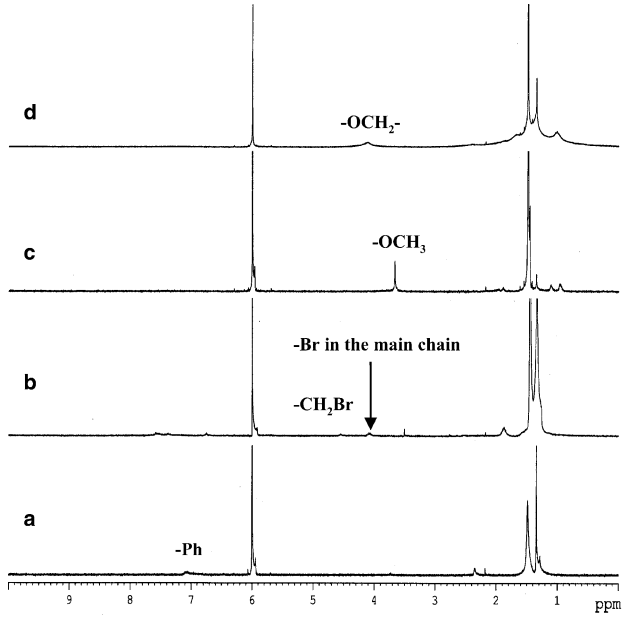

Fig. 4. The ^{1}H NMR spectra of: (a) PE-*co*-PMS; (b) PE-*co*-PMS bromination; (c) PE-*g*-PMMA; (d) PE-*g*-PBA.

the PMS units. The integrated intensity ratio between the chemical shift at 1.35 ppm and the chemical shifts between 7.0 and 7.3 ppm represent determines the components of PMS (the number of protons both chemical shifts).

Significantly, higher yield and activity were obtained in P[E-*co*-(*p*-MS)] compared to pure PE homopolymerization with similar reaction condition (B-1 and D-1 in Table 2). This phenomenon is because of the electronic donation from *p*-methyl substitution, which is extremely favorable in the cationic polymerization mechanism. Generally, the catalyst activity systematically increases with increasing of *p*-MS content. The *p*-methylstyrene has the "positive" comonomer effect in the ethylene copolymerization. Interestingly, a very large solvent (toluene and hexane) effect on the *rac*-Et(Ind)$_2$ZrCl$_2$ activity was observed in the comparative no. B-1/C-1 and D-3/E-1, despite the significant difference at the beginning of the reaction conditions (homogeneous in the toluene and heterogeneous in the hexane). The higher activity was obtained in the hexane by *rac*-Et(Ind)$_2$ZrCl$_2$/MAO catalyst. Under a similar reaction condition, *p*-MS incorporation is consistently higher in the toluene. This phenomenon may be due to the *p*-methylstyrene having a good dispersion in the aromatic solvent.

The P[E-*co*-(*p*-MS)] exhibits low melting point and small crystallinity, which implying a relatively random distribution of PMS along the polyethylene backbone. The detailed sequence distribution can be quantitatively determined by ^{13}C NMR measurements. Fig. 5 is the ^{13}C NMR spectrum of P[E-*co*-(*p*-MS)], which contain about 4.90 mol% of PMS. In the aromatic region (120–150 ppm), all of the chemical shifts agree closely with those aromatic carbons in PMS units, respectively. The sequence distribution is revealed by the chemical shifts corresponding to the carbons located along the polymer backbone. It is logical to expect that the methyl group substitution at the *para*-position will have little effect on the chemical shifts of methylene and methine carbons in the polymer backbone. Generally, every chemical shifts in Fig. 5 can easily be assigned. Additionally, the two chemical shifts (21.0 and 29.8 ppm)

Table 2
Properties of PE-*co*-PMS by using *rac*-Et(Ind)$_2$ZrCl$_2$ catalyst[a]

No.	Solvent (100 ml)	*p*-MS (mmol)	Yield (g)	Activity[b] ($\times 10^{-3}$)	PMS (mol%)	T_m (°C)	ΔH (J/g)	T_g (°C)	T_d (°C)
B-1	Toluene	–	1.46	4.8	–	133.3	242.5	–	480.6
C-1	Hexane	–	2.04	6.8	–	131.0	177.2	–	481.6
D-1	Toluene	10	1.52	5.1	1.1	124.3	136.5	–	473.9
D-2	Toluene	30	1.53	5.1	4.9	118.6	131.0	–	475.2
D-3	Toluene	90	2.03	6.7	7.4	114.2	106.6	−57.2	475.2
E-1	Hexane	90	3.03	10.1	6.1	107.9	111.1	−18.2	467.1

[a] *rac*-Et(Ind)$_2$ZrCl$_2$ = 10 μmol, MAO = 10 mmol, toluene = 100 ml, ethylene pressure = 40 psi, polymerization temperature = 40 °C, polymerization time = 1 h.
[b] Activity = kg product/(mol Zr × [C_2H_4] × h).

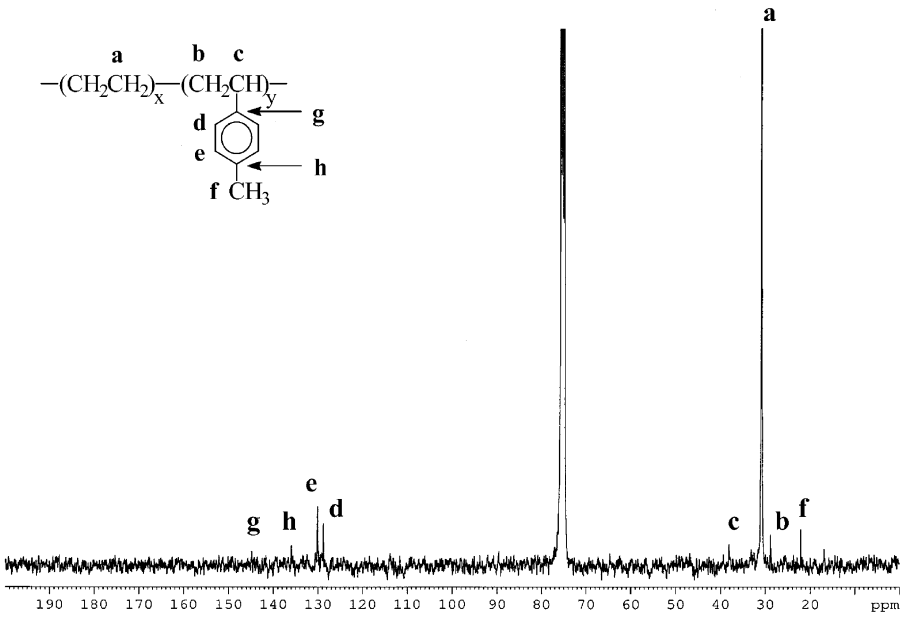

Fig. 5. The ^{13}C NMR spectrum of PE-*co*-PMS by using *rac*-Et(Ind)$_2$ZrCl$_2$ catalyst.

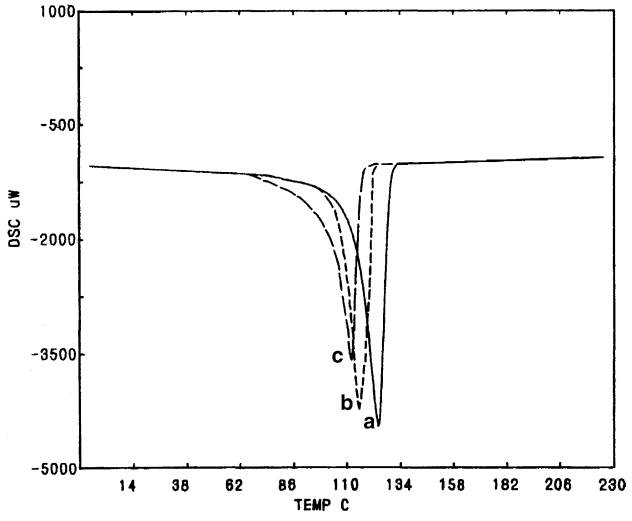

Fig. 6. The DSC curves of PE-*co*-PMS with PMS contents of: (a) 1.1; (b) 4.9; (c) 7.4 mol% by using *rac*-Et(Ind)$_2$ZrCl$_2$catalyst.

correspond to the methyl carbon from PMS and methylene carbons from ethylene, respectively. Three well-resolved peaks (27.7, 27.0 and 45.8 ppm) correspond to methylene and methine carbons from PMS units that are separated by multiple ethylene units along the polymer main chain.

Fig. 6 shows the comparison of DSC curves among different PMS components of P[E-*co*-(*p*-MS)] copolymers prepared by *rac*-Et(Ind)$_2$ZrCl$_2$ catalyst at 40 °C in toluene. A small amount of *p*-MS comonomer incorporation (about 1.1 mol%) significantly affects the crystallization of polyethylene (ΔH from 242.5 to 136.5 J/g). Moreover, the melting point and crystallinity of copolymer are strongly related to the component of the comonomer, with melting point and crystallinity decreasing with increasing component. If the PMS components were over 7.4 mol%, the glass transition temperature was occurred (at −57.2 °C) in the DSC curves. The lower decomposition temperature was obtained in the P[E-*co*-(*p*-MS)] from thermal gravimetric analysis (TGA) curves (decrease about 20 °C than PE). This phenomenon is because of the side group of PMS being decomposed in the low temperature.

3.2. Properties of polyethylene-g-poly(methylmethacrylate) and polyethylene-g-poly(t-butyl acrylate)

In this section, we will brominate of P[E-*co*-(*p*-MS)] as a halogen precursor. The P[E-*co*-(*p*-MS)] copolymer was mixed with *n*-bromosuccinimide (NBS) and 2,2′-azoisobutyronitrile (AIBN) in the carbon tetrachloride for proceeding the bromination reaction. Fig. 4(b) shows the ^1H NMR spectrum of bromination of P[E-*co*-(*p*-MS)] and the chemical shift of CH_2Br in the aromatic position occurs at 4.55 ppm. However, the methylene group in main chain will also be brominate by NBS and AIBN (at 4.1 ppm in the ^1H NMR). If this reaction was used higher NBS concentration or longer reaction time, more bromine groups would be contained in the main chain (over 50 mol%) to reduce the polyethylene original thermal properties (the melting point disappeared). But the bromine in the polymer backbone did not proceed the ATRP reaction because of the bond

Table 3
Properties of PE graft copolymers[a]

No.	Monomer (mmol)	Yield (g)	Insoluble[b] (g)	Copolmer[c] (mol%)	Graft length[d] (10^3g/mol)	T_m (°C)	ΔH (J/g)	T_g (°C)
F-1[b]	–	–	–	–	–	110.8	89.8	–
G-1	MMA (20)	0.88	0.73	7.2	24.09	–	–	106.6
G-2	MMA (40)	1.48	1.16	56.2	43.60	–	–	115.2
H-1	BA (20)	0.36	0.25	6.7	2.27	84.6	21.3	–
H-2	BA (40)	0.39	0.32	18.7	5.45	78.7	8.6	–

[a] Bromination PE-*co*-PMS = 0.2 g (Br = 2.2 mol%), CuCl = 1.0 mmol, bipy = 2.0 mmol, toluene = 40 ml, graft polymerization temperature = 100 °C, graft polymerization time = 24 h.
[b] The pure PE-*g*-PMMA and PE-*g*-PBA.
[c] Copolymer components in the graft copolymer were detected by ^{1}H NMR.
[d] Graft length = [(weight of graft copolymer) − (weight of bromination PE-*co*-PMS)]/(mole of CuCl).

strength being too strong. The CH_2Br group in the PMS unit is a good initiator (dormant alkyl halide) in the ATRP process.

CuCl/2,2-bipyridine was used as the metal catalyst and ligand compound for initiating ATRP reaction. The graft polymerizations were performed with methyl methacrylate (MMA) and *t*-butyl acrylate (BA). The ^{1}H NMR spectra indicate presence of both monomers in the final copolymers and enable quantitative determination of the amount of incorporated second monomer (Figs. 4(c) and (d)). The two additional chemical shifts arise at 3.5 ppm (Fig. 4(c)) and 4.1 ppm (Fig. 4(d)), corresponding to the OCH_3 and OCH_2 protons in the PMMA and PBA. The quantitative analysis of graft copolymers compositions was calculated by the ratio of two integrated intensities between these protons in the PMMA and PBA side chains and the methylene of protons ($\delta = 1.0$–2.0 ppm, the number of protons both chemical shifts represent).

Both the yield and graft components of the graft copolymer are basically proportional to the quantity of monomers used in the graft-from reaction. The good control of graft copolymer formation is obviously owing to the living/controlled ATRP polymerization which effectively converts monomers to the grafted side chains. In Table 3, the yield and PMMA (PBA) components increased with higher comonomer concentrations in the similar reaction condition. More MMA units were used to incorporate the P[E-*co*-(*p*-MS)] side chain (56.2 mol% at [MMA] = 40 mmol) because the MMA structure has less steric effect than BA. Under the same assumption of living free radical graft polymerization, the graft length (defined as the average molecular weight of side chain) can be estimated by the following equation [17]:

$$\text{Graft length(g/mol)} = \frac{\text{weight of graft copolymer} - \text{weight of bromination P[E-}co\text{-(}p\text{-MS)]}}{\text{mole of Br in the bromination P[E-}co\text{-(}p\text{-MS)]}},$$

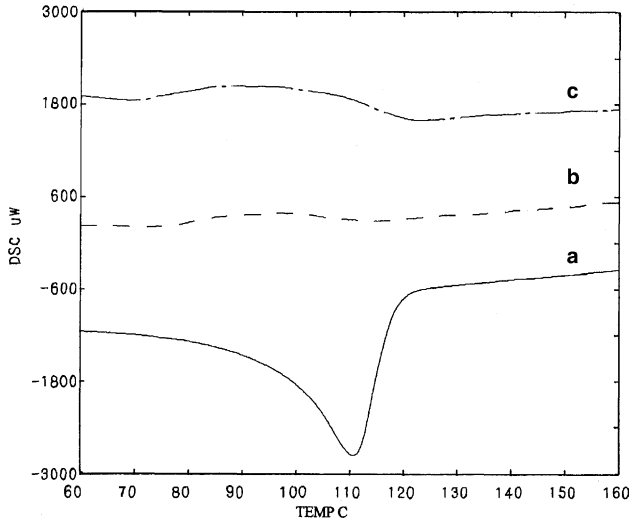

Fig. 7. The DSC curves of (a) PE-*co*-PMS and PE-*g*-PMMA with PMMA contents of (b) 7.2, (c) 56.2 mol%.

The molecular weight of the side chain is inversely proportional to the degree of radical form and the quantity comonomer used in the graft polymerization. Meanwhile, the graft length depends on the amount of graft comonomer incorporations into the side chain.

Figs. 7 and 8 show the DSC curves of PE-*g*-PMMA and PE-*g*-PBA to compare with P[E-*co*-(*p*-MS)], respectively. The PMMA units destroyed the crystallinity of polyethylene to make the melting point disappearance. The glass transition temperature of PE-*g*-PMMA could be obtained at 106.6 °C (no. F-1 in Table 3) and the glass transition temperature increased with increasing incorporation of MMA comonomer. On the other hand, the PBA units just decreased the melting point and enthalpy of polyethylene. This phenomenon was related

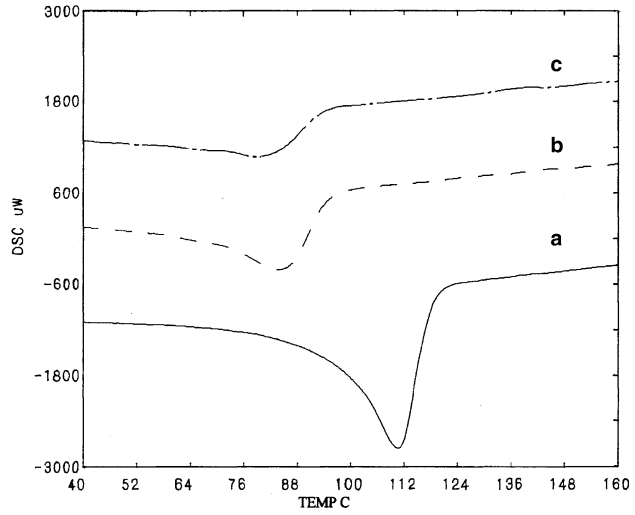

Fig. 8. The DSC curves of (a) PE-*co*-PMS and PE-*g*-PBA with PBA contents of (b) 6.7, (c) 18.7 mol%.

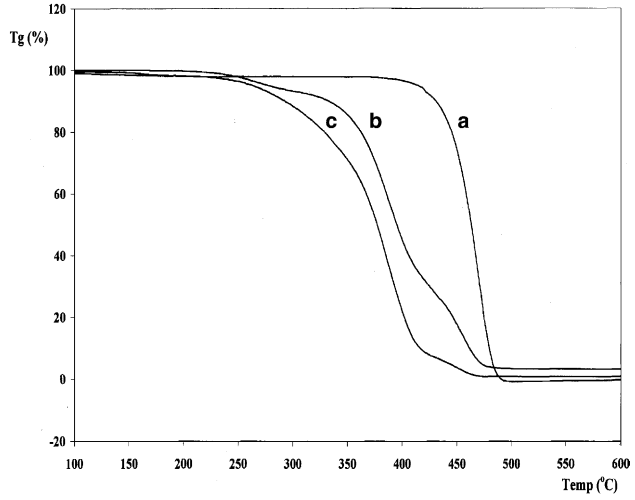

Fig. 9. The TGA curves of: (a) PE-*co*-PMS; (b) PE-*g*-PMMA; (c) PE-*g*-PBA.

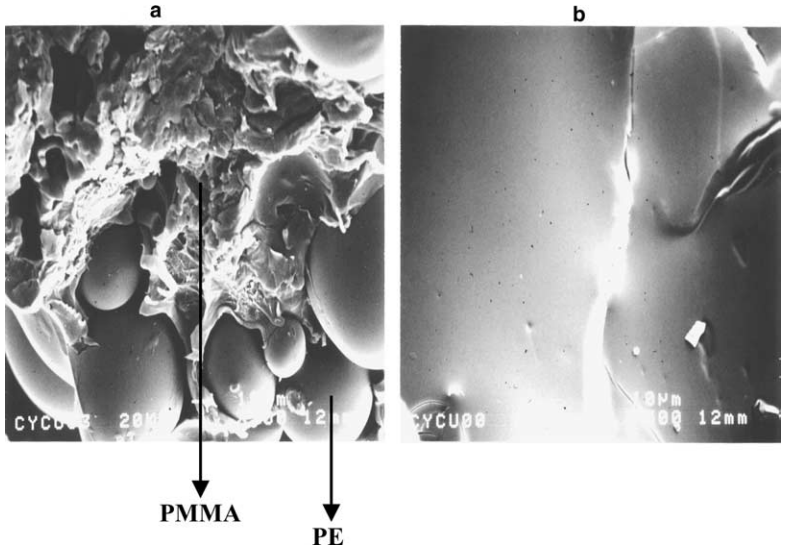

Fig. 10. The SEM micrographs of: (a) PE/PMMA blend [50/50 wt%]; (b) PE/PMMA/PE-*g*-PMMA blend [50/50/20 wt%].

with the graft length and copolymer composition, the higher PBA units the lower melting point and enthalpy. The decomposition temperature could be observed from the TGA curves in Fig. 9. Thermal degradation of PE graft copolymers involves two distinct steps. The first is due to decomposition of the side chain of copolymer and the second is the polyethylene main chain. The longer side chain breaks the arrangement and crystallinity of polyethylene and the graft form copolymer clearly exhibits decomposition temperature than P[E-*co*-(*p*-MS)].

Studying the compatibility of PE-*g*-PMMA copolymer in HDPE and PMMA blends is of interest. The SEM was used to examine the bulk morphologies shown in Fig. 10. Two blends comprised an overall 50/50 weight ratio of PE and PMMA, one was a simple 50/50 mixture of HDPE and PMMA and the other was a 50/50/20 weight ratio of HDPE, PMMA and PE-*g*-PMMA (containing 56.2 mol% of PMMA). Fig. 10 shows the SEM micrographs, which is the surface topography of cold-fractured lump edges. In the homopolymer blend, the polymers are grossly phase-separated as can be seen by the PMMA component that exhibits nonuniform, poorly dispersed domains and voids at the fracture surface, as shown in Fig. 10(a). This baal and socket topography indicates of poor interfacial adhesion between the PE and PMMA domains and represents PMMA domains that are pulled out of the PE matrix. Such pull out indicates that limited stress transfer takes place between phases during fracture. The similar blend containing graft copolymer shows a totally different morphology in the Fig. 10(b). The material exhibits flat mesa-like regions similar to pure PE. No distinct PMMA phases are observable, indicating that

fracture occurred through either phase or that the PMMA phase domains are too small to be observed. The PE-*g*-PMMA is clearly proven to be an effective compatibilizer in the PE/PMMA blends.

4. Conclusions

This study discusses the copolymerization reaction of ethylene and *p*-methylstyrene (MS) via the homogeneous metallocene catalyst, *rac*-Et(Ind)$_2$ZrCl$_2$. With increasing *p*-methylstyrene concentration, the poly[ethylene-*co*-(*p*-methylstyrene)] copolymer exhibits systematical reduction of melting temperature and crystallinity and increase of glass temperature. Using the bromination reaction of poly[ethylene-*co*-(*p*-methylstyrene)], polyethylene-*g*-poly(methylmethacrylate) and polyethylene-*g*-poly(*t*-butyl acrylate) could be prepared via atomic transfer radical polymerization. The following selective bromination reaction of *p*-methylstyrene units in the copolymer and the subsequent radical graft-from polymerization were effective methods of producing polymeric side chains with well-defined structures. In the bulk, the individual PE and PMMA segments in the graft copolymers are phase-separated to form crystalline PE domains and amorphous PMMA domains. The SEM micrographs studies display the effectiveness of PE-*g*-PMMA in the polymer blends by reducing phase sizes, improving dispersion and increasing interfacial interaction between domains.

References

[1] M.D. Baijal, Plastics polymer science and technology, Wiley, New York, 1982.
[2] E.C. Carraher, J.A. Moore, Modification of polymers, Plenum, Oxford, 1982.
[3] J. Boor, Ziegular-Natta catalysts and polymerization, Academic Press, New York, 1979.
[4] G. Ruggeri, M. Aglietto, A. Petragnani, F. Ciardelli, Eur. Polym. J. 19 (1983) 863.
[5] J.W. Eshuis, Y.Y. Tan, A. Meetsma, J.H. Teuben, J. Renkema, G.G. Evens, Organometallics 11 (1992) 362.
[6] J.K. Johnson, S. Mecking, M. Brookhart, J. Am. Chem. Soc. 118 (1996) 267.
[7] M.R. Kesti, G.W. Coates, R.M. Waymouth, J. Am. Chem. Soc. 114 (1992) 9679.
[8] G. Riess, J. Periard, A. Manderet, Colloidal and morphological behavior of block and graft copolymer, Plenum Press, New York, 1971.
[9] D.J. Lohse, S. Datta, E.N. Kresge, Macromolecules 24 (1991) 561.
[10] T.C. Chung, D. Rhubright, G.J. Jiang, Macromolecules 26 (1993) 3467.
[11] G.J. Jiang, D. Rhubright, R.L. Bernard, T.C. Chung, Polym. Mater. Sci. Eng. 205 (1993) 22.
[12] G.J. Jiang, T.C. Chung, C.L. Li, Macromolecules 27 (1994) 26.
[13] G.J. Jiang, T.C. Chung, W. Janvikul, R. Bernard, R. Hu, C.L. Li, S.L. Liu, Polymer 36 (1995) 3565.
[14] G.J. Jiang, T.Y. Wang, J. Chin. Chem. Soc. 45 (1998) 341.
[15] G.J. Jiang, J.M. Hwu, S.F. Lee, M.T. Hsu, J. Chin. Chem. Soc. (2000).
[16] T.C. Chung, H.L. Lu, J. Polym. Sci. Part A: Polym. Chem. 35 (1997) 575.
[17] T.C. Chung, H.L. Lu, R.D. Ding, Macromolecules 30 (1997) 1272.
[18] T.C. Chung, H.L. Lu, J. Polym. Sci. Part A: Polym. Chem. 36 (1998) 1017.
[19] T.C. Chung, H.L. Lu, S. Hong, J. Polym. Sci. Part A: Polym. Chem. 37 (1999) 2795.
[20] I. Piirma, J.R. Lenzotti, Brit. Polym. J. 21 (1989) 45.
[21] F. Bonaccorsi, A. Lezzi, A. Prevedello, L. Lanzini, A. Roggero, Polym. Int. 30 (1993) 93.
[22] L.P. Ferrari, H.D. Stover, Macromolecules 24 (1991) 6340.
[23] J.S. Wang, K. Matyjaszewski, J. Am. Chem. Soc. 117 (1995) 5614.
[24] D.P Curran, B.M. Trost, I.Des. FlemingComprehensive organic synthesis, vol. 4, Pergamon, Oxford, 1991, p. 715.
[25] J.H. Udding, K.J.M. Tuijp, M.N. Zanden, H. Hiemstra, W.N. Speckamp, J. Org. Chem. 59 (1994) 1993.
[26] J.S. Wang, K. Matyjaszewski, J. Am. Chem. Soc. 117 (1995) 5614.
[27] J. Xia, X. Zhang, K. Matyjaszewski, Macromolecules 32 (1999) 3531.